Vitamin A aldehyde-taurine adduct and the visual cycle

Hye Jin Kim[a], Jin Zhao[a], and Janet R. Sparrow[a,b,1]

[a]Department of Ophthalmology, Columbia University Medical Center, New York, NY 10032; and [b]Department of Pathology and Cell Biology, Columbia University Medical Center, New York, NY 10032

Edited by Jeremy Nathans, The Johns Hopkins University School of Medicine, Baltimore, MD, and approved August 31, 2020 (received for review March 30, 2020)

Visual pigment consists of opsin covalently linked to the vitamin A-derived chromophore, 11-*cis*-retinaldehyde. Photon absorption causes the chromophore to isomerize from the 11-*cis*- to all-*trans*-retinal configuration. Continued light sensitivity necessitates the regeneration of 11-*cis*-retinal via a series of enzyme-catalyzed steps within the visual cycle. During this process, vitamin A aldehyde is shepherded within photoreceptors and retinal pigment epithelial cells to facilitate retinoid trafficking, to prevent nonspecific reactivity, and to conserve the 11-*cis* configuration. Here we show that redundancy in this system is provided by a protonated Schiff base adduct of retinaldehyde and taurine (A1-taurine, A1T) that forms reversibly by nonenzymatic reaction. A1T was present as 9-*cis*, 11-*cis*, 13-*cis*, and all-*trans* isomers, and the total levels were higher in neural retina than in retinal pigment epithelium (RPE). A1T was also more abundant under conditions in which 11-*cis*-retinaldehyde was higher; this included black versus albino mice, dark-adapted versus light-adapted mice, and mice carrying the Rpe65-Leu450 versus Rpe65-450Met variant. Taurine levels paralleled these differences in A1T. Moreover, A1T was substantially reduced in mice deficient in the Rpe65 isomerase and in mice deficient in cellular retinaldehyde-binding protein; in these models the production of 11-*cis*-retinal is compromised. A1T is an amphiphilic small molecule that may represent a mechanism for escorting retinaldehyde. The transient Schiff base conjugate that the primary amine of taurine forms with retinaldehyde would readily hydrolyze to release the retinoid and thus may embody a pool of 11-*cis*-retinal that can be marshalled in photoreceptor cells.

photoreceptor cells | retinal pigment epithelium | vitamin A | visual cycle | taurine

Vitamin A aldehyde is present in retina as both *cis* and *trans* isomers. The light-sensitive 11-*cis*-retinaldehyde (11cisRAL) chromophore in both rod and cone photoreceptor cells is covalently bound to opsin proteins by protonated Schiff base (PSB) linkage. In this capacity, the chromophore absorbs photons of light to begin the process of phototransduction. Following photon capture, 11-*cis*-retinal is converted to the all-*trans* configuration and is released from the binding pocket of opsin. Continued photon capture requires regeneration of the 11-*cis* chromophore by one or more multistep processes. One of these pathways, the canonical visual cycle, consists of enzymes residing in photoreceptor cells and the adjacent retinal pigment epithelium (RPE). Although retinaldehyde molecules are critical to vision, they are also hydrophobic and highly reactive. To facilitate the movement of retinoids through the visual cycle and to prevent nonspecific chemical reaction the visual cycle utilizes multiple mechanisms for handling these molecules when they are not sequestered within the binding pockets of opsin (1). For example, multiple species of dehydrogenases are available to reduce retinaldehydes; these enzymes, by converting the aldehyde to an alcohol, limit the quantities of retinaldehyde (2, 3). Additionally, the aqueous soluble carrier cellular retinaldehyde-binding protein (CRALBP) in RPE and Müller cells chaperones 11cisRAL, thereby reducing product inhibition of the isomerase activity, maintaining the *cis*-isomer state of 11-*cis*-retinal and protecting against the reactivity of the aldehyde (4–8).

All-*trans*-retinal released from photoactivated opsin can be picked up by neighboring phosphatidylethanolamine (PE) in the disk membrane, thereby forming the reversible Schiff base, *N*-retinylidene-PE (NRPE) (9–11), that sequesters the reactive aldehyde and may enable nonenzymatic visual pigment renewal (11, 12). NRPE is also recognized as the ligand that binds the photoreceptor-specific ATP-binding cassette transporter (ABCA4) in outer segments (13–19). The function of ABCA4 is to transport nonprotonated NRPE across the lipid bilayer from the interior of the disk to the cytoplasmic face of the disk membrane, where all-*trans*-retinaldehyde (atRAL) is released and subsequently reduced to the less reactive alcohol (all-*trans*-retinol) by NADPH-dependent retinol dehydrogenases (RDH8, RDH11, and RDH12) (2, 18, 20–23). The 11-*cis* isomer of NRPE (*N*-11-*cis*-retinylidene-PE) can also be transported by ABCA4 from the inner disk to the cytoplasmic leaflet of disk membranes; this is a role that is presumed to prevent excess levels of 11-*cis*-retinal (17, 20).

Inefficient removal of the NRPE isomers is a hazard since this Schiff base conjugate can react with a second molecule of all-*trans*-retinal instead of hydrolyzing to PE and all-*trans*-retinal. This second irreversible condensation reaction is the first step in a nonenzymatic synthetic pathway leading to the formation of fluorescent di-retinal compounds within the lipid bilayers of the photoreceptor outer segment. These compounds include the phosphatidyl-pyridinium bisretinoid, A2PE; the pyridinium bisretinoids A2E and A2-GPE; the phosphatidyl-dihydropyridine bisretinoid, A2-DHP-PE; and both all-*trans*-retinal dimer and the related PE conjugate, all-*trans*-retinal dimer-PE (20, 24). Phagocytosis of shed outer segments by RPE results in the accumulation of these toxic compounds in RPE cells.

It was recognized a number of years ago that retinaldehyde also combines with the endogenous sulfur-containing amino acid

Significance

Taurine is a sulfur-containing amino acid that is not incorporated into protein but is abundant in retina. Schiff base adducts that form nonenzymatically and reversibly from reactions between taurine and vitamin A aldehyde (A1T) are increased under conditions in which the visual chromophore 11-*cis*-retinal is more abundant. These settings include black versus albino mice, dark-adapted versus light-adapted mice, and mice expressing the Rpe65-Leu450 versus Rpe65-Met450 variant. Conversely, A1T is less abundant in mouse models deficient in 11-*cis*-retinal. As an amphiphile, protonated A1T may serve to facilitate retinoid trafficking and could constitute a small-molecule reserve of mobilizable 11-*cis*-retinal in photoreceptor cells.

Author contributions: H.J.K. and J.R.S. designed research; H.J.K. and J.Z. performed research; H.J.K. and J.R.S. analyzed data; and H.J.K. and J.R.S. wrote the paper.

The authors declare no competing interest.

This article is a PNAS Direct Submission.

[1]To whom correspondence may be addressed. Email: jrs88@cumc.columbia.edu.

This article contains supporting information online at https://www.pnas.org/lookup/suppl/doi:10.1073/pnas.2005714117/-/DCSupplemental.

First published September 21, 2020.

taurine to produce the taurine-retinaldehyde Schiff base, A1-taurine (A1T) (25) (Fig. 1). Taurine contains a sulfonic acid group in place of the typical carboxylic group of an amino acid and it carries a primary amine. Taurine is not incorporated into protein but in a study of 110 metabolites representative of all major metabolic pathways, only uptake of proline by RPE was greater than taurine (26). Although taurine is abundant in neural retina, its function is poorly understood and little or no attention is paid to A1T. Here we sought to understand the physiological significance of A1T in retina.

Results

A1T Isomers in Synthetic Mixtures. Given its conjugated double bonds, retinaldehyde ($C_{20}H_{28}O$, molecular weight [MW] 285.4) can exist in multiple isomeric forms that include 9-*cis*, 11-*cis*, 13-*cis*, and all-*trans* isomers. The all-*trans*, 9-*cis*, and 13-*cis* isomers are thermodynamically more stable than 11-*cis*-retinal. We began this work by analyzing the products of cell-free biosynthetic reactions between taurine ($C_2H_7NO_3S$, MW 125.2) and all-*trans*-retinal and with the *cis*-isomers of retinaldehyde (Fig. 1). On the basis of UV-visible absorbance spectra, retention times and selected ion monitoring of mass (protonated, *m/z* 392.6), we identified all-*trans*-A1T (maximum absorption wavelength, λ_{max} 448 nm), and the *cis*-isomers of A1T, 11-*cis*-A1T (λ_{max} 450 nm), 9-*cis*-A1T (λ_{max} 440 nm), and 13-*cis*-A1T (λ_{max} 440 nm), in ultraperformance liquid chromatography (UPLC) chromatograms (Fig. 2).

The maximum absorption wavelength (λ_{max}) of the non-protonated retinal Schiff base NRPE is 365 nm (12, 21). With protonation of the nitrogen, the absorbance maximum red shifts to 455 nm (9, 12, 17, 21). Under the acidic conditions of our chromatography we observed that A1T had a λ_{max} of 450 nm. With spectrometric recording of the absorbance of synthetic all-*trans*-A1T in methanol at neutral pH, λ_{max} was also 450 nm (*SI Appendix*, Fig. S1); this indicated that A1T exists as a PSB in both a neutral and acidic environment. We note that *n*-butylamine retinal-Schiff bases (*N*-retinylidene-*n*-butylamine) have a dissociation constant (pK_a) from 6 to 7 (27) and the pK_a of NRPE is 6.9 (21). Thus A1T (*N*-retinylidene-taurine) is expected to have a relatively high pK_a due to the negatively charged sulfonated group that can delocalize electrons and thereby stabilize the nearby N-H bond.

Photo- and Thermal Isomerization of A1T Species. The presence of A1T as a PSB is also of interest since protonation of an all-*trans* Schiff base promotes efficient nonenzymatic *trans-cis* isomerization

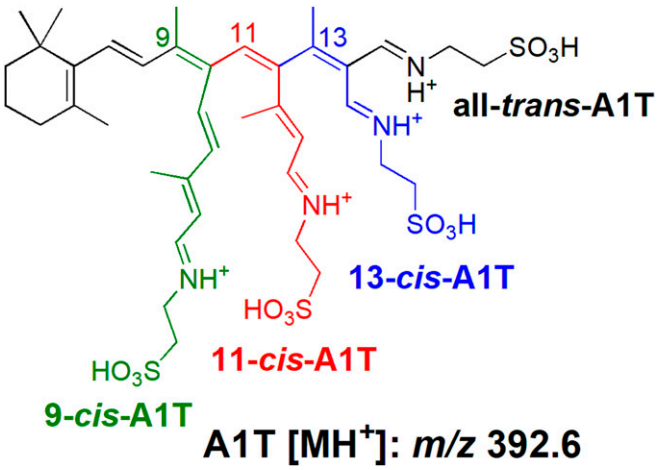

Fig. 1. Structures of 9-*cis* (green), 11-*cis* (red), 13-*cis* (blue) A1T, and all-*trans*-A1T (black) (A1T; *N*-retinylidene-taurine) shown as protonated forms with protonated mass (*m/z* 392.6).

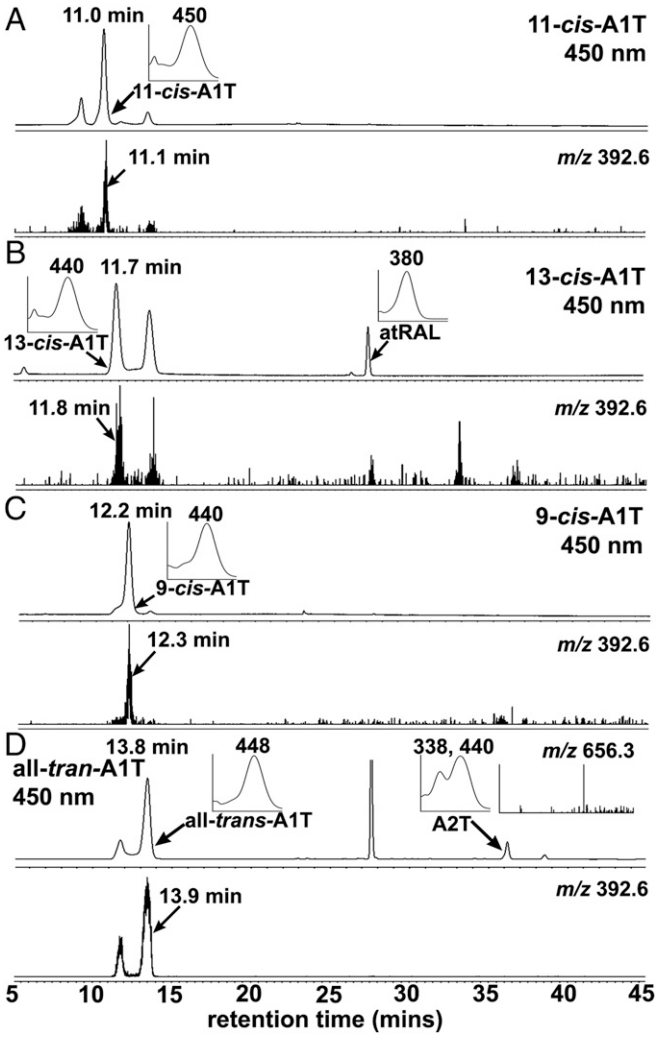

Fig. 2. Chromatographic detection of synthetic A1-taurine (A1T) isomers produced by incubating taurine with retinaldehyde isomers. A1T isomers (11-*cis*, 9-*cis*, and 13-*cis*-A1T; and all-*trans*-A1T). Separation by UPLC-UV/Vis-ESI-MS with absorbance detected at 450 nm (*Upper* traces in *A–D*) and selected ion monitoring (SIM) at *m/z* 392.6 (*Lower* traces in *A–D*). Retention times in minutes. (*Insets*) UV/visible absorbance maxima (λ_{max}) corresponding to indicated peaks (arrows). (*A*) 11-*cis*-A1T: retention time 11.0 min; λ_{max}, 450 nm; SIM at *m/z* 392.6 with retention time11.1 min. (*B*) 13-*cis*-A1T: retention time 11.7 min; λ_{max}, 440 nm; SIM at *m/z* 392.6 with retention time 11.8 min; all-*trans*-retinal (atRAL): retention time 28.0 min, λ_{max}, 380 nm. (*C*) 9-*cis*-A1T: retention time 12.2 min, *m/z* 440 nm; SIM at *m/z* 392.6 with retention time 12.3 min. (*D*) all-*trans*-A1T: retention time 13.8 min, λ_{max}, 448 nm; SIM at *m/z* 392.6 with retention time 13.9 min. A2T: retention time 36.2 min, λ_{max}, 338, 440 nm, MS spectrum at *m/z* 656.3.

(12, 28). Thus, we tested for evidence of interconversion of A1T isomers (11-*cis*, 9-*cis*, 13-*cis*-A1T, and all-*trans*-A1T) using synthesized samples of each A1T isomer, dehydrated conditions (methanol), and exposure durations of 1 and 13 h (room light, 75 lx; room temperature) (Fig. 3). As shown in the table in Fig. 3*D*, exposures of 9-*cis*-A1T, 11-*cis*-A1T, and all-*trans*-A1T isomers followed by UPLC analysis of the photoproducts revealed retention times and absorbances consistent with photoconversion to all four isomers (11-*cis*-A1T, 9-*cis*-A1T, 13-*cis*-A1T, all-*trans*-A1T) (Fig. 3 *A–C*). Examination of the ratios of these isomers indicated that all-*trans*-A1T was the most favored configuration after illumination; next was 9-*cis*-A1T. Configurational isomerism to 11-*cis*-A1T was observed in all cases (Fig. 3*D*).

To examine the thermal interconversion of A1T isomers, 11-*cis*-A1T was incubated at 37 °C for 1 h, 19 h, and 64 h in the dark (*SI Appendix*, *SI Methods*). Visual inspection of the chromatographic peaks attributable to 11-*cis*-A1T and all-*trans*-A1T in *SI Appendix*, Fig. S2 revealed that isomerization of 11-*cis*-A1T to the lower-energy all-*trans*-A1T is only appreciable after 19 h (*SI Appendix*, *SI Results* and Fig. S2). This protracted time-line indicates that 11-*cis*-A1T exhibits greater thermal stability than photostability (Fig. 3 *B* and *D* and *SI Appendix*, Fig. S2).

A1T Is Detected in Human Retina. To circumvent Schiff base formation during the extraction process, a biphasic system was utilized to impose the separation of retinaldehyde and taurine. Moreover, protonation of the primary amine of taurine in acidified methanol rendered the latter incapable of nucleophilic attack on the aldehyde (*SI Appendix*, *SI Methods*, *SI Results*, and Fig. S3). Under these conditions A1T, the reversible Schiff base adduct of one retinaldehyde and taurine, was detected in human retina by UPLC (Fig. 4 *A* and *B*). A1T was present as the 11-*cis*-, 13+9-*cis*-, and all-*trans*-A1T isomers (Fig. 4*B*); identification was based on absorbance spectra and retention times corresponding to synthetic standards (Fig. 4*A*). The A1T isomers were readily detected in neural retina (Fig. 4*B*). Although under synthetic conditions with the aid of base catalysis, we detected A2T, the nonreversible condensation product of taurine with 2 vitamin A aldehyde (retention time 36.2 min; λ_{max} 338, 440) (Fig. 4*A*), in the human retina A2T was not detected (Fig. 4*B*).

***Trans*- and *cis*-isomers of A1T in Mouse Retina.** We quantified A1T isomers by integration of peak areas, adjustment to standard curves constructed for each isomer and normalization to the internal standard, A1-*β*-alanine (*SI Appendix*, Fig. S4). In cyclic light-reared black C57BL/6J murine eyes, A1T was detected in extracts of neural retina but not in RPE (Fig. 4 *C*–*E*). Moreover, in isolated neural retina the A1T isomers all-*trans*-A1T, 13-*cis*/9-*cis*-A1T, and 11-*cis*-A1T were present (Fig. 4 *C*–*E*). The absorbance maxima of these isomers (all-*trans*-A1T, 448 nm; 11-*cis*-A1T, 450 nm; 9-*cis*-A1T, 440 nm; 13-*cis*-A1T, 440 nm) in methanol were consistent with that of protonated retinal Schiff base conjugates (28, 29). Based on the retention time of A2T (36.2 min), A2T was not detected in the mouse retina (Fig. 4 *D* and *E*).

Retinoid, A1T, and Ocular Pigmentation. In the absence of ocular melanin, light entering the eye is substantially increased (30–32). To compensate for increased photon catch, albino mice have reduced rhodopsin content (photostasis) (33). Consistent with the principles of photostasis, we observed lower levels of 11-*cis*-retinal and 11-*cis*-retinol (11cisROL) in eyes of albino C57BL/6J^{c2j} mice as compared to black C57BL/6J mice ($P < 0.0001$ for 11-*cis*-retinal, $P < 0.01$ for 11-*cis*-retinol, two-way ANOVA, Sidak's multiple comparison test) (Fig. 5 *A* and *B*). Except for the tyrosinase gene, these mice have the same genetic background. All-*trans*-retinal was higher in albino C57BL/6J^{c2j} mice than in black C57BL/6J mice ($P < 0.0001$, two-way ANOVA). As expected, atRAL was also higher in all light-adapted mice (regardless of strain) than in dark-adapted mice (Fig. 5*A*). No differences were observed in all-*trans*-retinol, all-*trans*-retinyl esters (atRE), and 11-*cis*-retinyl esters (11cisRE) based on pigmentation (Fig. 5 *A* and *B*).

Total A1T levels paralleled the albino-black differences in 11-*cis*-retinal under cyclic light conditions. Thus, total A1T was approximately threefold lower in the albino C57BL/6J^{c2j} mice than in the black C57BL/6J mice ($P < 0.0001$, two-way ANOVA with Sidak's multiple comparison test) (Fig. 5*C*). The 11-*cis*-A1T isomer was only detected in light-adapted black C57BL/6J mice; this isomer was undetectable in albino C57BL/6J^{c2j} and albino BALB/cJ housed in cyclic light (Fig. 5*C*).

Cyclic Light and Dark Adaptation. During a period of darkness, the isomerization of 11-*cis*-retinal to all-*trans*-retinal is arrested due to the absence of photons and full visual sensitivity is restored due to regeneration of light-absorbing 11-*cis*-retinal. Thus 11-*cis*-retinal was significantly greater in dark-adapted (18 h) albino C57BL/6J^{c2j} and BALB/cJ mice (age 2 mo) than in the corresponding mice housed in continuous cyclic light (12-h on, 12-h off; $P < 0.0001$, two-way ANOVA, Sidak's multiple comparison test) (Fig. 5*A*). Conversely, in all three mouse strains (C57BL/6J, C57BL/6J^{c2j}, and BALB/cJ), all-*trans*-retinal was significantly lower ($P < 0.0001$, two-way ANOVA) in the dark-adapted versus

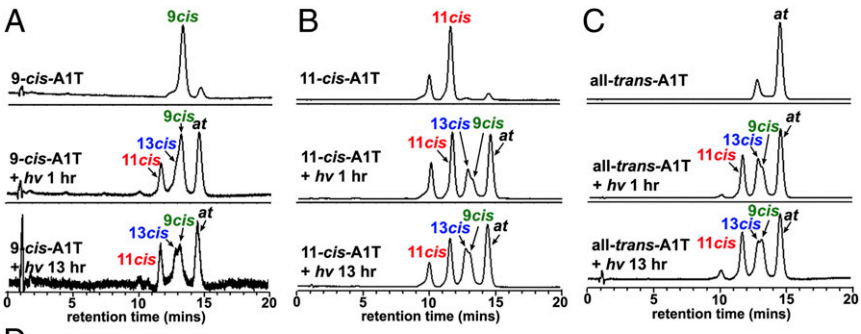

D

starting isomer	ratio after light (1 hr)			ratio after light (13 hr)		
	11-*cis*-A1T	9+13-*cis*-A1T	all-*trans*-A1T	11-*cis*-A1T	9+13-*cis*-A1T	all-*trans*-A1T
9-*cis*-A1T*	1	2.8	2.6	1	2	2
11-*cis*-A1T*	1.6	1	1.8	1	1.2	1.4
all-*trans*-A1T*	1	1.8	2.2	1	1.8	2.2

Fig. 3. Photoisomerization of A1-taurine isomer (A1T). UPLC-UV/Vis detection of A1T isomers at 450 nm before and 1 h and 13 h after 9-*cis*-A1T (*A*), 11-*cis*-A1T (*B*), and all-*trans*-A1T (*C*) were exposed to light (*hv*). (*D*) Starting isomers (with asterisk) in methanol and ratios of A1T isomers after light exposure. Given their absorption maxima (~440 and 450 nm in methanol), all A1T isomers correspond to the protonated Schiff base.

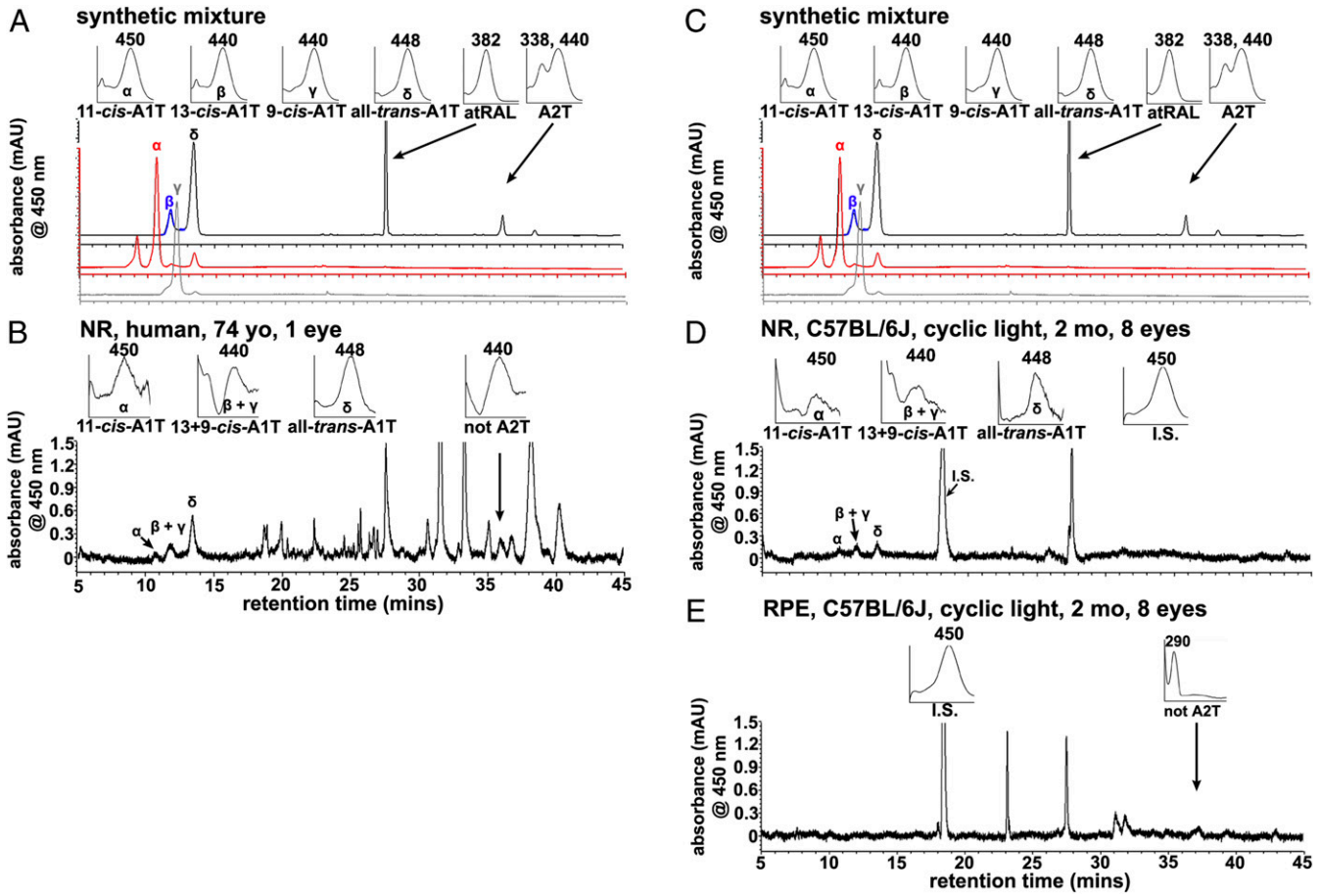

Fig. 4. Chromatographic detection of A1T in human and mouse retina. A1T is more abundant in mouse neural retina (NR) than in RPE. Separation by UPLC with monitoring at 450 nm. (*A* and *C*) Detection of synthetic products derived from incubation of retinaldehyde isomers with taurine: The panels in *A* and *C* present synthesized A1T isomers: 11-*cis*-A1T, red trace; combined 13-*cis*-A1T, and all-*trans*-A1T, blue and black traces, respectively; 9-*cis*-A1T, gray trace. UV/Vis absorbance maximum, λ_{max}. (*Insets*) UV/visible (Vis) absorbance spectra corresponding to indicated peaks (α–δ, arrows). 11-*cis*-A1T (α): λ_{max} 450 nm, retention time 11.0 min; 13-*cis*-A1T (β): λ_{max}, 440 nm, retention time 11.7 min; 9-*cis*-A1T (γ): λ_{max}, 440 nm, retention time 12.2 min; all-*trans*-A1T (δ): λ_{max} 448 nm, retention time 13.8 min; A2T, λ_{max}, 338, 440 nm, retention time 36.2 min. (*B*) Human neural retina (NR). The UPLC injectant was a methanolic extract of neural retina (age 74 y). 11-*cis*-A1T: λ_{max},450 nm, retention time 11.0 min; 13+9-*cis*-A1T: λ_{max}, 440 nm, retention time 11.8~12.2 min; all-*trans*-A1T: λ_{max} 448 nm, retention time 13.8 min. (*C*) To enable alignment with other panels, chromatograms in *A*, repeated in *C*, are the same as in *A*. (*D*) Cyclic light-reared black C57BL/6J mice, NR (age 2 mo, 8 eyes, 30.2 mg wet weight). The UPLC injectant was a methanolic extract of neural retina. 11-*cis*-A1T (α): λ_{max} 450 nm, retention time 11.0 min, 13 + 9-*cis*-A1T: λ_{max}, 440 nm, retention time 11.8 ~ 12.2 min. all-*trans*-A1T: λ_{max}, 448 nm, retention time 13.8 min. I.S. (internal standard, A1-*β*-alanine): λ_{max}, 450 nm, retention time 18.0 min. (*E*). RPE harvested from cyclic light-reared black C57BL/6J mice, (age 2 mo, 8 eyes, 19.3 mg wet weight). No A1T isomers were detected in RPE. I.S. (internal standard, A1-*β*-alanine): λ_{max}, 450 nm, retention time 18.0 min. The unknown peaks (*B* and *E*) at retention time 36.2 min exhibits λ_{max}, 440 and 290 nm. These peaks do not correspond to A2T, the latter being produced in the synthetic mixture presented in *A* and *C*. Although the retention times are similar to A2-taurine (retention time 36.2 min), they present with a single λ_{max} (440 nm, 290 nm) in the sample of NR. Conversely, A2T has 2 absorbance maxima (λ_{max} 338, 440 nm). This unknown peak is likely NRPE (λ_{max}).

light-adapted mice. The latter difference reflects reduced photoisomerization of 11-*cis*-retinal in darkness (Fig. 5*A*).

A difference in 11-*cis*-retinal levels between light and dark adaptation in the black C57BL/6J mice was not observed, probably due to the density of melanin in these mice. However, all-*trans*-retinal was higher in the light-adapted mice ($P < 0.0001$, two-way ANOVA) (Fig. 5*A*). Differences in all-*trans*-retinol and all-*trans*-retinyl ester levels as a function of ocular pigmentation and dark versus light adaptation were not observed (Fig. 5*A*). Levels of 11cisRE were greater in dark-adapted C57BL/6J^{c2j} than in light-adapted C57BL/6J^{c2j} mice ($P < 0.05$, two-way ANOVA) (Fig. 5*B*).

As with the differences exhibited by 11cisRAL, total A1T was significantly greater in the dark-adapted (18 h) albino C57BL/6J^{c2j} (11.00 ± 0.74; 2.0-fold, $P < 0.0001$) and BALB/cJ (16.72 ± 2.07, 2.3-fold, $P < 0.0001$) mice relative to the cyclic light-adapted C57BL/6J^{c2j} mice (5.42 ± 1.23) and BALB/cJ mice (7.16 ± 0.81; two-way ANOVA, Sidak's multiple comparison test) (Fig. 5*C*). Levels of 11-*cis*-A1T were lower than the detection limit in cyclic light-reared albino mice (C57BL/6J^{c2j}); but the mean levels were 7.45 ± 0.71 pmoles per eye under dark-adapted conditions (Fig. 5*C*). Combined 13-*cis*-A1T/9-*cis*-A1T was not detected in either dark- or light-adapted albino mice (C57BL/6J^{c2j}, BALB/cJ) but was detected in black C57BL/6J mice (Fig. 5*C*). The A1T isomer 11-*cis*-A1T was detectable in cyclic light-housed black C57BL/6J mice but undetectable in cyclic light-housed albino C57BL/6J^{c2j} mice (Fig. 5*C*). NRPE was also more abundant in dark-adapted C57BL/6J^{c2j} mice as compared to mice maintained in cyclic light ($P < 0.0001$, *t* test) (Fig. 5*D*).

We note that total A1T levels tracked 11-*cis*-retinaldehyde and not all-*trans*-retinal levels. For example, in C57BL/6J^{c2j} and BALB/cJ mice, 11-*cis*-retinaldehyde was present at higher levels in dark-adapted versus light-adapted mice. Similarly, total A1T

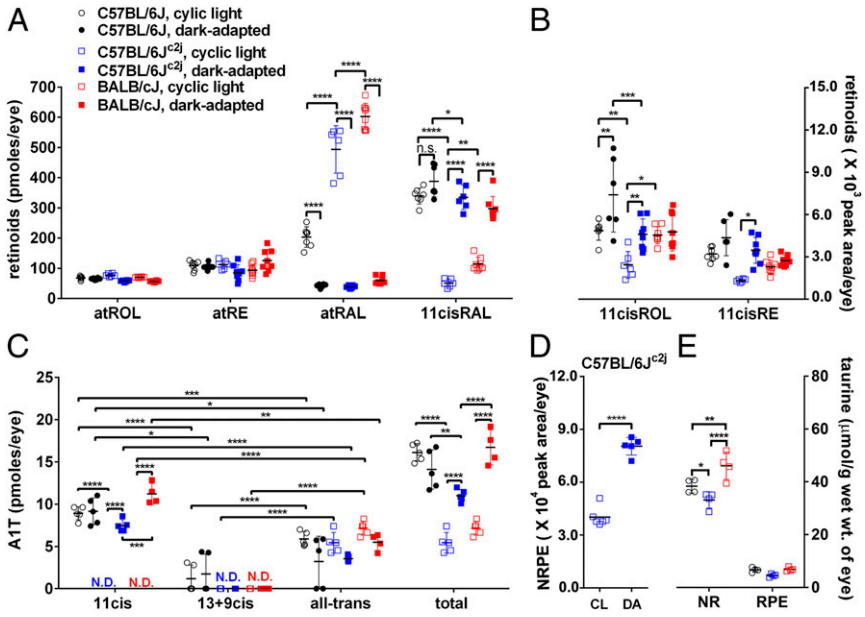

Fig. 5. UPLC quantitation of retinoids, A1T isomers, NRPE, and HPLC quantitation of taurine in mouse eyes. Mice varying with respect to coat color (black, albino), Rpe65-Leu450 versus Rpe65-450Met variant and under continuous cyclic light (CL) versus dark adaptation (DA). Individual values, means ± SD. (*A*) Retinoids (atROL, atRE, atRAL, 11cisRAL). (*B*) 11cisROL and 11cisRE in black C57BL/6J, albino C57BL/6J^{c2j}, albino BALB/cJ mice (age 2 mo) and with continuous light versus dark adaptation. One eye per sample, $n = 6$–8 samples. In the absence of calibration curves for 11cisROL and 11cisRE quantitation is presented as peak areas. (*C*) A1T isomers in black C57BL/6J, albino C57BL/6J^{c2j}, albino BALB/cJ mice (age 2 mo) in continuous cyclic light or dark adaptation. Four eyes per sample, $n = 4$ to 5 samples. N.D., not detected. (*D*) NRPE in albino C57BL/6J^{c2j} mice (age 2 mo) under continuous cyclic light versus dark adaptation, two eyes per sample, $n = 6$ samples. (*E*) Taurine levels in isolated neural retina and RPE of black C57BL/6J (Rpe65-450Met), albino C57BL/6J^{c2j} (Rpe65-450Met); albino BALB/cJ (Rpe65-Leu450). Mice were housed in cyclic light until age 2 mo. Individual values, means ± SD; $n = 4$ samples (two eyes per sample). *P* values were determined by two-way ANOVA and Sidak's multiple comparison test (*A*–*C*), Tukey's multiple comparison test (*E*). To compare A1T isomers in the same mouse line, *P* values were determined by one-way ANOVA and Tukey's multiple comparison test (*C*). For NRPE comparison, *P* values were determined by two-tailed *t* test (*D*). *$P < 0.05$, **$P < 0.01$, ***$P < 0.001$, ****$P < 0.0001$.

was 2.0- and 2.3-times ($P < 0.0001$ for C57BL/6J^{c2j}, $P < 0.0001$ for BALB/cJ mice, two-way ANOVA, Sidak's multiple comparison test) more abundant in dark-adapted (18 h) versus light-adapted mice. The greatest difference was in 11-*cis*-A1T. In BALB/cJ mice the latter increased from nondetection (under cyclic light) to 11.22 pmol per eye (under dark adaptation), while 13-*cis*-A1T/9-*cis*-A1T remained nondetected and all-*trans*-A1T showed no significant difference in dark-adapted versus mice continuously reared in cyclic light ($P < 0.0001$ for 11-*cis*-A1T; two-way ANOVA, Sidak's multiple comparison test) (Fig. 5*C*).

Rpe65-Leu450Met Polymorphism. There are likely numerous genetic polymorphisms distinguishing BALB/cJ mice from the C57BL/6J^{c2j} strain (34). One functionally relevant variant resides in the isomerase Rpe65, whereby in the C57BL/6J and C57BL/6J^{c2j} mice methionine replaces leucine at amino acid 450 (Rpe65-Leu450Met) such that the regeneration of 11-*cis*-retinal is retarded (32, 35, 36). BALB/cJ mice express the wild-type form (Rpe65-Leu450). Accordingly, we found that levels of 11-*cis*-retinal, 11-*cis*-retinol, and all-*trans*-retinal were significantly lower in the cyclic light-adapted albino C57BL/6J^{c2j} mice than in the albino BALB/cJ mice ($P < 0.0001$ for atRAL, $P < 0.01$ for 11cisRAL; $P < 0.05$ for 11cisROL, two-way ANOVA, Sidak's multiple comparison test) (Fig. 5 *A* and *B*). In dark-adapted albino C57BL/6J^{c2j} (Rpe65-450Met) mice, 11-*cis*-retinal levels were not significantly different from in BALB/cJ mice (Rpe65-Leu450) ($P > 0.05$, two-way ANOVA, Sidak's multiple comparison test) (Fig. 5*A*), probably because the period of darkness allows the slower visual cycle in the C57BL/6J^{c2j} mice to achieve parity. Differences in the levels of A1T were observed. Specifically, in cyclic light-adapted and dark-adapted (18 h) mice, those mice carrying the Rpe65-450Met variant (albino C57BL/6J^{c2j}) exhibited reduced total A1T as compared to the Rpe65-Leu450 variant (BALB/cJ) ($P < 0.0001$, comparison of dark-adapted mice; $P > 0.05$, comparison between light-adapted mice). Moreover, while 11-*cis*-A1T was not detected in light-adapted albino C57BL/6J^{c2j} and BALB/cJ mice, in the dark-adapted cohorts 11-*cis*-A1T was lower in the presence of the 450Met variant (C57BL/6J^{c2j}) ($P < 0.001$, two-way ANOVA, Sidak's multiple comparison test) (Fig. 5*C*).

Rpe65-Null Mutant Mice. After photon absorption the visual chromophore 11cisRAL must be regenerated by the isomerase Rpe65 of the visual cycle to recover light sensitivity (37–39). In *Rpe65*$^{-/-}$ mice atREs accumulate in the RPE cells and 11-*cis*-retinoids are absent (40). In our studies 11-*cis*-A1T, 13+9-*cis*- and all-*trans*-A1T were not detected in cyclic light-housed *Rpe65*^{rd12} mice (Fig. 6*A*).

A1T in CRALBP Mutant Mice. RPE and Müller cells express CRALBP that is encoded by the gene *RLBP1*. CRALBP binds 11-*cis*-retinol produced by RPE65 thereby facilitating the oxidation of 11-*cis*-retinol to 11-*cis*-retinal by retinol dehydrogenase 5 (RDH5) (1). Deletion of CRALBP does not block the production of 11-*cis*-retinoid, however CRALBP-null mutant mice (41, 42) exhibit delayed dark adaptation due to reduced Rpe65 activity. Thus, the role of CRALBP in the visual cycle is to accelerate production of 11-*cis*-retinoid. To examine for effects of inefficient 11-*cis*-retinal recycling, we measured A1T levels in *Rlbp1*/Cralbp$^{-/-}$ mice. Total A1T was reduced in agouti *Rlbp1*/Cralbp$^{-/-}$ versus agouti wild-type control mice ($P < 0.0001$, two-way ANOVA and Sidak's multiple comparison test) (Fig. 6*B*). The reduction in 11-*cis*-A1T and all-*trans*-A1T were also significant

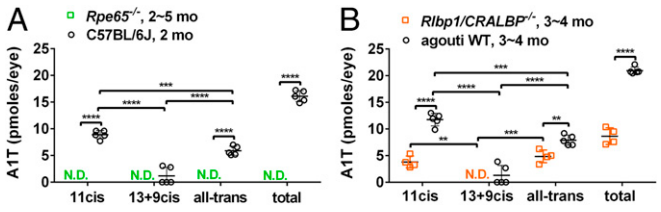

Fig. 6. UPLC quantitation of A1T isomers in mice housed in cyclic light. Individual values, means ± SD (*A*) A1T isomers in *Rpe65*$^{-/-}$ (2 ~ 5 mo, 4 eyes per sample, $n = 4$ samples) and C57BL/6J mice (age 2 mo, 4 eyes per sample, $n = 4$). N.D., not detected. (*B*) A1T isomers in *Rlbp1*/Cralbp$^{-/-}$ (age 3 ~ 4 mo, 4 eyes per sample, $n = 4$) and agouti WT mice (age 3 ~ 4 mo, 4 eyes per sample, $n = 5$). To compare each A1T isomers in mutant versus wild-type mice, *P* values were determined by two-way ANOVA and Sidak's multiple comparison test (*A* and *B*). To compare A1T isomers in the same mouse line: *P* values were determined by one-way ANOVA and Tukey's multiple comparison test (*A* and *B*). $^{**}P < 0.01$, $^{***}P < 0.001$, $^{****}P < 0.0001$.

($P < 0.0001$ for 11-*cis*-A1T; $P < 0.01$ for all-*trans*-A1T, two-way ANOVA and Sidak's multiple comparison test) (Fig. 6*B*).

Taurine Levels in Wild-Type Mice. In the mouse, endogenous taurine was detected in both RPE and neural retina but the levels were seven- to eightfold higher in neural retina (Fig. 5*E*). In isolated neural retina but not in RPE, taurine levels were higher in cyclic light-reared albino BALB/cJ mice ($P < 0.0001$, two-way ANOVA with Tukey's multiple comparison test) that express the Rpe65-Leu450 variant versus albino C57BL/6J^{c2j} mice and black C57BL/6J mice that carry the Rpe65-450Met ($P < 0.01$; two-way ANOVA) variant that slows the visual cycle (Fig. 5*E*). An effect of pigmentation was also noted: Taurine was more abundant in the neural retina of black C57BL/6J mice than in albino C57BL/6J^{c2j} mice ($P < 0.05$, two-way ANOVA) (Fig. 5*E*).

Discussion

Absorption of a photon of light leads to the isomerization of 11-*cis*-retinal to all-*trans*-retinal. To restore photosensitivity, the all-*trans*-isomer is reconverted to 11-*cis*-retinal. During these multistep processes, provisions must be made to protect against nonspecific reactivity of the aldehyde; to aid trafficking of lipophilic retinaldehyde by conferring water solubility (43); and ultimately, to maintain the 11-*cis* configuration. These issues have been addressed by mechanisms that sequester and chaperone retinaldehyde (44). Here we demonstrate that additional redundancy in this system is provided by the nonenzymatic reversible formation of a Schiff base adduct between retinaldehyde and the primary amine of taurine. We propose that A1T contributes to the sequestration and chaperoning of retinaldehyde, with the formation of A1T being transient as it would hydrolyze to release retinaldehyde (Fig. 7). Indeed, in contrast to the retinaldehyde-PE conjugate NRPE, which can react with a second retinaldehyde to generate irreversible and undesirable bisretinoid fluorophores, the product of a second condensation reaction involving A1T and retinaldehyde was not detected in mouse or human retina. NRPE, the Schiff base of retinaldehyde and PE, can exist in either a protonated or unprotonated state (45). The unprotonated form of NRPE binds to ABCA4, the transporter in photoreceptor outer segments that aids in delivering retinaldehyde in the form of NRPE to the retinol dehydrogenase on the cytoplasmic side of the disk membrane (21). Additionally, since as a nucleophile NRPE requires a pair of free electrons to attack the aldehyde, it is expected to be unprotonated (nucleophilic enamine) when it reacts with a second retinaldehyde to irreversibly form bisretinoids (24), the fluorescent compounds that constitute the lipofuscin of retina. Conversely, absorbance wavelengths we have recorded for A1T indicate that A1T is a protonated adduct. This state may explain the absence of A2T in the eye.

There are other differences between NRPE and A1T. For example, NRPE bears hydrophobic long-chain fatty acids and is expected to exist in a hydrophobic environment. On the other hand, A1T is an amphiphilic small molecule carrying a negatively charged sulfonated group together with a hydrophobic retinoid moiety (Fig. 1); as such, A1T may represent a mechanism in photoreceptor cells for escorting retinaldehyde, a molecule that is otherwise poorly soluble in an aqueous milieu. As noted above, NRPE is the ligand that is recognized by ABCA4 in its effort to remove reactive retinaldehyde from photoreceptors after photon absorption. NRPE has also been suggested to function in the photoregeneration of visual pigment by light-dependent conversion of all-*trans*-NRPE to its 11-*cis* isomer (46).

Taurine and total A1T were both higher in neural retina than in RPE. In wild-type albino mice total A1T was also more abundant under conditions in which 11-*cis*-retinal was present at relatively higher levels. For example, elevated total A1T accompanied the increase in 11-*cis*-retinal associated with dark adaptation. Here the greatest difference was observed in 11-*cis*-A1T. Total A1T was also increased with black versus albino ocular pigmentation and in albino mice carrying the Rpe65-Leu450 variant (BALB/cJ) relative to the Rpe65-450Met variant (C57BL/6J^{c2j} mice). Conversely, none of the A1T isomers were detected in *Rpe65*$^{-/-}$ mice in which 11-*cis*-retinal is not produced. Less pronounced but significantly reduced total A1T, 11-*cis*-A1T, and all-*trans*-A1T were observed in *Rlbp1*/Cralbp$^{-/-}$ mice exhibiting a less-severe impairment in 11-*cis*-retinal production relative to wild-type.

The classic visual cycle residing in photoreceptors and RPE is well known to provide 11-*cis*-retinal to both rods and cones

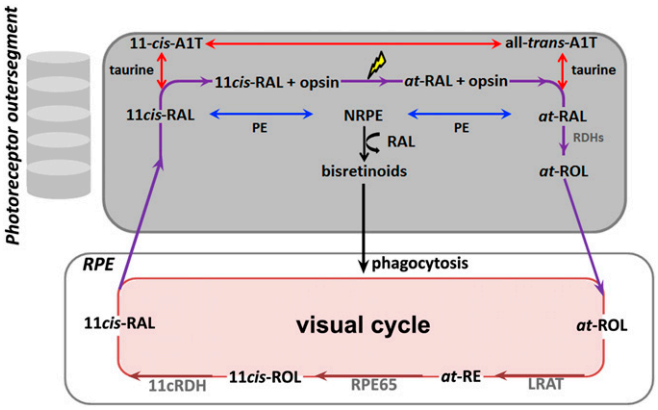

Fig. 7. A schematic illustrating the proposed role of A1T in retina. Vision is initiated in photoreceptor cell outer segments when opsin is activated by a photon causing the 11-*cis* chromophore to isomerize to the all-*trans* configuration. To begin the process of regeneration of 11-*cis*-retinal (11*cis*-RAL), all-*trans*-retinaldehyde (at-RAL) is reduced to all-*trans*-retinol (*at*-ROL) either directly or after reaction of *at*-RAL with PE in the disk membrane of photoreceptor outer segments; NRPE that forms is transported by ABCA4 to the cytosolic compartment of the outer segment, where it hydrolyzes and *at*-RAL is reduced by retinol dehydrogenases (Rdhs). Alternatively, some *at*-RAL and 11*cis*-RAL reacts with taurine to form A1T. A1T would readily hydrolyze to release RAL and taurine and interconversion of A1T isomers (11-*cis*-A1T between all-*trans*-A1T) could occur. Bisretinoids form randomly in outer segments when NRPE reacts nonenzymatically with a second molecule of retinaldehyde (RAL); bisretinoid fluorophores ultimately accumulate in RPE by phagocytosis of photoreceptor outer segment. The visual cycle is completed within RPE: LRAT converts at-ROL to all-*trans*-retinyl esters (at-RE); the isomerase RPE65 generates 11-*cis*-retinol (11*cis*-ROL), and 11*cis*-ROL is oxidized to 11*cis*-RAL by 11-*cis*-retinol dehydrogenase (11cRDH).

(47–50). Studies of animal models and human vision have repeatedly shown, however, that to sustain photosensitivity in daylight, cones must have access to an additional source of 11-*cis*-retinal beyond that provided by the classic visual (retinoid) cycle. These mechanisms may involve Müller glia, RPE cells, or both, and they may be light-dependent pathways involving RGR (retinal G protein-coupled receptor) with all-*trans*-retinal as substrate (51) or light-independent processes that harness the retinoid isomerase isomerase sphingolipid δ(4)-desaturase 1 (DES1) (46, 49). It remains to be determined which, if any of these processes, A1T can serve. The high concentration of taurine in retina (52) is likely consistent with concentrations that would be necessary for an efficient scavenger of retinaldehyde.

There are numerous indications that the function of taurine in retina relates in large part to photoreceptor cells. For example, taurine levels are higher in photoreceptor cells than in inner retina (53). In cats (54) raised on a diet that depletes serum and retinal levels of taurine (55, 56) and in mice carrying a deletion in the SLC6a6Tau gene encoding for TauT, severe photoreceptor degeneration is observed (57). On the other hand, taurine is reported to attenuate light-induced damage to photoreceptor cells (58, 59). There is also a precipitous decrease in taurine accompanying photoreceptor cell degeneration in the postnatal rd1 and C3H mouse (53, 60). Destruction of inner retina has a minimal effect on the quantity of taurine, while in photoreceptorless mice taurine levels are drastically reduced. We also note that taurine (52) (Fig. 5*E*) and A1T quantities are particularly high in mouse neural retina relative to RPE (Fig. 4). Taurine abundance is also nearly 10-fold greater than other amino acids (52). Although taurine is primarily acquired in the diet, its biosynthesis from cysteine and methionine can also occur (52, 53).

The Schiff base adduct between retinaldehyde and taurine, A1T, can exist in multiple isomeric forms that include 9-*cis*, 11-*cis*, 13-*cis*, and all-*trans* isomers (Fig. 4). Levels of total A1T and 11-*cis*-A1T tended to track levels of 11-*cis*-retinal in retina. No configurational changes were observed with 11-*cis*-A1T before and after extraction, suggesting isomerization did not occur during the extraction process for A1T (*SI Appendix*, Fig. S5). We detected 9-*cis* and 13-*cis*-A1T in pigmented mice under conditions in which 9-*cis* and 13-*cis*-retinaldehyde are very low in amount (12, 46, 49, 61). For example, the isomer 9-*cis*-retinal may constitute only 0.2% of visual chromophore in wild-type mice (46). On the one hand, taurine may form adducts with 9-*cis*, 13-*cis*, and atRAL isomers previously generated by isomerization of the 11-*cis*-configuration. The retinol isomerase Rpe65 (62) and DES1 in Müller glia (46) are both reported to produce small amounts of 13-*cis*-retinol; DES1 is also a source of 9-*cis*-retinol (46). In Rpe65-null mutant mice reared under prolonged dark-adapted conditions, 9-*cis*-retinal can accumulate, bind opsin, photoisomerize to all-*trans*-retinal, and re-enter the visual cycle (61). CRALBP exhibits binding to not only 11-*cis*-retinol and 11-*cis*-retinal but also 9-*cis*-retinoids (but not all-*trans* or 13-*cis*-retinoids) (4, 63). On the other hand, 13-*cis*-retinol, once formed, can be oxidized to 13-*cis*-retinal but it is not used as visual chromophore, nor does it accumulate in healthy eyes (46). Thus, whether 13-*cis*-retinal re-enters the visual cycle is not known. The all-*trans* retinoid species are the most stable with 11-*cis* isomer being of higher energy. The high double-bond isomerization barrier is a significant obstacle to a spontaneous change in configuration to the 11-*cis*-isomer within the rhodopsin molecule (64, 65). However, several studies have reported that the activation energy required for isomerism of a PSB is considerably smaller than that of retinoids and smaller than that of an unprotonated retinal Schiff base (3.1 ∼ 5.2 kcal/mol for isomerization of PSB of retinal) (66–68). Thus, the low-energy barrier introduced by taurine could help in making interconversion of each isomer of A1T possible. Accordingly, we observed here that when bound by a Schiff base linkage to taurine, the barrier to isomerization is reduced and isomerization to 11-*cis*, 9-*cis*, and 13-*cis*-A1T is observed in the presence of light.

There are several unknowns. For example, how are A1T levels modulated in response to shifts in taurine availability such as could occur due to inhibition of taurine transport? Interest in taurine has been intensified by reports that photoreceptor cell degeneration occurring as a side-effect of the antiepileptic drug vigabatrin (GABA-transaminase inhibitor) is due to taurine depletion (52, 69, 70). One might wonder whether the handling of retinaldehyde by taurine is involved in this toxicity. Moreover, to what extent do the findings reported here apply to both rods and cones? Involvement of A1T in a cone-driven visual cycle could explain the low levels of 11-*cis*-A1T in mouse given that in this rodent only 5% of photoreceptor cells are cones. Little is known regarding the handling of 11-*cis*-retinal within a hydrophilic environment of photoreceptor outer segments after its delivery across the subretinal space from RPE to photoreceptors. A1T may represent a hydrophilic pool of readily mobilizable 11-*cis*-retinal in photoreceptor cells. During the process of dark adaptation (34), this source of 11-*cis*-retinal would not be rate-limiting as it would not depend on the time involved in delivery of 11-*cis*-retinal from RPE.

Materials and Methods

Mouse Models and Human Tissue. BALB/cJ, C57BL/6J, C57BL/6J^{c2j}, 129S1/SvImJ mice and *Rpe65*^{rd12} were purchased from Jackson Laboratories. Cralbp$^{-/-}$ mice (Rpe65-Leu450; agouti) were obtained as a gift from Vladimir J. Kefalov, Ophthalmology & Visual Sciences, Washington University School of Medicine in St. Louis, St. Louis, MO, and were bred in-house. Mice were homozygous for the Rpe65-Leu450 or Rpe65-Met450 variant (71) as indicated. In-cage illumination was 30 to 80 lx. To achieve dark-adapted conditions, mice were placed in darkness for 18 h. Genotyping for the rd8 mutation in *Crb1* using previously described primers and protocol (48) confirmed that the mutant mice do not carry the rd8 mutation. The research was approved by the Institutional Animal Care and Use Committee of Columbia University and was performed in accordance with the Association for Research in Vision and Ophthalmology Statement for the Use of Animals in Ophthalmic and Visual Research. A human donor eye (age 74 y) was received within 24 h of death from the Eye Bank for Sight Restoration (New York, NY). The study was in accordance with the Declaration of Helsinki with regard to the use of human tissue.

Synthesis of A1T Species and A2T. The 9-*cis*-retinal, 13-*cis*-retinal, and all-*trans*-retinal were purchased from Sigma-Aldrich. The 11-*cis*-retinal was a gift from the National Eye Institute, provided through the laboratory of Rosalie K. Crouch. A1T isomers were synthesized by reacting 9-*cis*, 11-*cis*, 13-*cis*, and all-*trans* isomers of retinaldehyde with taurine (1:1 molar ratio of retinal isomers and taurine) in dehydrated methanol containing sodium methoxide (72). To synthesize A2T, the product of reaction of taurine with 2 retinaldehyde, a twofold molar excess of atRAL was added to the same reaction mixture. All of the isomers of A1T were purified in their protonated forms by HPLC with a reverse-phase Atlantis Prep dC18 column (10 × 250 mm, 10 μm; Waters) and gradient of acetonitrile and water with 0.1% TFA.

Tissue Extraction and Quantitative UPLC Analysis of Retinoids. Frozen mouse eyecups (one eye per sample) were carefully homogenized with 1 mL of *O*-ethylhydroxylamine (100 mM) in DPBS (pH 6.5, without $CaCl_2$ and $MgCl_2$) on ice under dim red light. After vortexing, samples were incubated for 15 min at 4 °C. All-*trans*-retinyl acetate (internal standard) and methanol (1 mL) were added to the samples and the latter were extracted with hexane (three times). After centrifugation (1,500 × *g* for 5 min at 4 °C), the hexane phase was evaporated under argon gas and then dissolved in 20 μL of acetonitrile for UPLC analysis (73, 74). Retinoids extracted from ocular tissues were analyzed and quantified as previously described (73).

UPLC Detection of A1T Isomers. Whole or isolated neural retina and isolated RPE/choroid from murine and human eyes (four to eight eyes for mice and one eye for human per sample) were homogenized in acidified MeOH (0.1% TFA) and extracted in chloroform/DPBS (2:1.3) on ice and under dim red light. A1-β-alanine, as internal standard (*SI Appendix, SI Methods* and Fig. S4) was added to compensate for the loss of endogenous A1T due to hydrolysis of

the Schiff base. The sample was then centrifuged (5 min, 1,500 × *g*, 4 °C), and filtered, and the extraction repeated twice by addition of chloroform (*SI Appendix, SI Methods, SI Results,* and Fig. S3). The combined chloroform fraction was dried under Ar gas and then redissolved in MeOH and measured by Waters Acquity UPLC system. UPLC analysis was performed using an XBridge BEH C18 column (2.5 μm, 3.0 × 50 mm) with detection at 450 nm. A1-taurine isomers 11-*cis*, 13-*cis*, 9-*cis*, and all-*trans*-retinal were separated with water and acetonitrile, both with 0.1% formic acid (0 to 15 min, 40% acetonitrile; 15 to 25 min, 40 to 75% acetonitrile; 25 to 45 min, 75 to 85% acetonitrile; 45 to 55 min, 85 to 100% acetonitrile and the final condition was held for 15 min) at 0.5 mL/min. Each isomer of A1T was identified by comparison of retention times with synthetic standards and quantification was performed using calibration curves. To calculate total A1T, the isomers were quantified separately and then summed.

HPLC Quantitation of Taurine. Isolated neural retina and isolated RPE/choroid were homogenized in DPBS and extracted with chloroform and methanol (1:1) to exclude the hydrophobic fraction after measuring the wet weight. The DPBS fraction was derivatized with NBD-F solution (1 mmol/L) as described previously (75). HPLC analysis was carried out using a Waters Alliance system with a fluorescence detector (excitation: 470 nm, emission: 530 nm). An Atlantis T3 C18 column (5 μm, 4.6 × 250 mm) was used with a mobile phase of MeOH/acetonitrile (1:1) and 10 mM ammonium acetate at pH 6.5 (0 to 15 min, 97% 10 mM ammonium acetate; 15 to 30 min, 97 to 85% 10 mM ammonium acetate; flow rate of 0.8 mL/min). Quantification of taurine was performed using standard curves.

Photoisomerization of A1T Species. Twenty micromolar of A1T isomers (9-*cis*-A1T, 11-*cis*-A1T, and all-t*rans*-A1T) in dehydrated methanol were exposed to room light (75 lx) and temperature for 1 h and 13 h. A1T isomers were analyzed by UPLC with monitoring at 450 nm before and after light exposure.

Statistical Analysis. Statistical analysis was carried out using GraphPad Prism 8.0 and $P < 0.05$ was considered significant.

Data Availability. All study data are included in the article and supporting information.

ACKNOWLEDGMENTS. This work was supported by grants from the National Eye Institute (EY024091 and EY012951; and P30EY019007) and Research to Prevent Blindness to the Department of Ophthalmology, Columbia University.

1. J. C. Saari, Vitamin A and vision. *Subcell. Biochem.* **81**, 231–259 (2016).
2. J. D. Chrispell *et al*., Rdh12 activity and effects on retinoid processing in the murine retina. *J. Biol. Chem.* **284**, 21468–21477 (2009).
3. A. Maeda *et al*., Redundant and unique roles of retinol dehydrogenases in the mouse retina. *Proc. Natl. Acad. Sci. U.S.A.* **104**, 19565–19570 (2007).
4. X. He, J. Lobsiger, A. Stocker, Bothnia dystrophy is caused by domino-like rearrangements in cellular retinaldehyde-binding protein mutant R234W. *Proc. Natl. Acad. Sci. U.S.A.* **106**, 18545–18550 (2009).
5. R. Parker, J. S. Wang, V. J. Kefalov, R. K. Crouch, Interphotoreceptor retinoid-binding protein as the physiologically relevant carrier of 11-cis-retinol in the cone visual cycle. *J. Neurosci.* **31**, 4714–4719 (2011).
6. J. C. Saari, D. L. Bredberg, Photochemistry and stereoselectivity of cellular retinaldehyde-binding protein from bovine retina. *J. Biol. Chem.* **262**, 7618–7622 (1987).
7. J. C. Saari, J. W. Crabb, Focus on molecules: Cellular retinaldehyde-binding protein (CRALBP). *Exp. Eye Res.* **81**, 245–246 (2005).
8. H. Stecher, M. H. Gelb, J. C. Saari, K. Palczewski, Preferential release of 11-cis-retinol from retinal pigment epithelial cells in the presence of cellular retinaldehyde-binding protein. *J. Biol. Chem.* **274**, 8577–8585 (1999).
9. R. E. Anderson, M. B. Maude, Phospholipids of bovine outer segments. *Biochemistry* **9**, 3624–3628 (1970).
10. R. P. Poincelot, P. G. Millar, R. L. Kimbel Jr., E. W. Abrahamson, Lipid to protein chromophore transfer in the photolysis of visual pigments. *Nature* **221**, 256–257 (1969).
11. H. Shichi, R. L. Somers, Possible involvement of retinylidene phospholipid in photoisomerization of all-trans-retinal to 11-cis-retinal. *J. Biol. Chem.* **249**, 6570–6577 (1974).
12. J. J. Kaylor *et al*., Blue light regenerates functional visual pigments in mammals through a retinyl-phospholipid intermediate. *Nat. Commun.* **8**, 16 (2017).
13. J. Ahn, J. T. Wong, R. S. Molday, The effect of lipid environment and retinoids on the ATPase activity of ABCR, the photoreceptor ABC transporter responsible for Stargardt macular dystrophy. *J. Biol. Chem.* **275**, 20399–20405 (2000).
14. M. Illing, L. L. Molday, R. S. Molday, The 220-kDa rim protein of retinal rod outer segments is a member of the ABC transporter superfamily. *J. Biol. Chem.* **272**, 10303–10310 (1997).
15. L. L. Molday, A. R. Rabin, R. S. Molday, ABCR expression in foveal cone photoreceptors and its role in Stargardt macular dystrophy. *Nat. Genet.* **25**, 257–258 (2000).
16. D. S. Papermaster, B. G. Schneider, M. A. Zorn, J. P. Kraehenbuhl, Immunocytochemical localization of a large intrinsic membrane protein to the incisures and margins of frog rod outer segment disks. *J. Cell Biol.* **78**, 415–425 (1978).
17. F. Quazi, R. S. Molday, ATP-binding cassette transporter ABCA4 and chemical isomerization protect photoreceptor cells from the toxic accumulation of excess 11-cis-retinal. *Proc. Natl. Acad. Sci. U.S.A.* **111**, 5024–5029 (2014).
18. H. Sun, R. S. Molday, J. Nathans, Retinal stimulates ATP hydrolysis by purified and reconstituted ABCR, the photoreceptor-specific ATP-binding cassette transporter responsible for Stargardt disease. *J. Biol. Chem.* **274**, 8269–8281 (1999).
19. H. Sun, J. Nathans, Stargardt's ABCR is localized to the disc membrane of retinal rod outer segments. *Nat. Genet.* **17**, 15–16 (1997).
20. H. J. Kim, J. R. Sparrow, Bisretinoid phospholipid and vitamin A aldehyde: Shining a light. *J. Lipid Res.*, 10.1194/jlr.TR120000742 (2020).
21. F. Quazi, S. Lenevich, R. S. Molday, ABCA4 is an N-retinylidene-phosphatidylethanolamine and phosphatidylethanolamine importer. *Nat. Commun.* **3**, 925 (2012).
22. G. H. Travis, M. Golczak, A. R. Moise, K. Palczewski, Diseases caused by defects in the visual cycle: Retinoids as potential therapeutic agents. *Annu. Rev. Pharmacol. Toxicol.* **47**, 469–512 (2007).
23. R. S. Molday, ATP-binding cassette transporter ABCA4: Molecular properties and role in vision and macular degeneration. *J. Bioenerg. Biomembr.* **39**, 507–517 (2007).
24. J. R. Sparrow *et al*., The bisretinoids of retinal pigment epithelium. *Prog. Retin. Eye Res.* **31**, 121–135 (2012).
25. A. M. Petrosian *et al*., New HPLC evidence on endogenous tauret in retina and pigment epithelium. *Adv. Exp. Med. Biol.* **483**, 453–460 (2000).
26. J. R. Chao *et al*., Human retinal pigment epithelial cells prefer proline as a nutrient and transport metabolic intermediates to the retinal side. *J. Biol. Chem.* **292**, 12895–12905 (2017).
27. A. M. Schaffer, T. Yamaoka, R. S. Becker, Visual pigments. V. Ground and excited-state acid dissociation constants of protonated all-trans retinal Schiff base and correlation with theory. *Photochem. Photobiol.* **21**, 297–301 (1975).
28. K. Freedman, R. S. Becker, D. Hannak, E. Bayer, Investigation into the spectroscopy and photoisomerization of a series of poly(ethylene glycol) peptide Schiff bases of 11-cis retinal. *Photochem. Photobiol.* **43**, 291–295 (1986).
29. D. S. Kliger, S. J. Milder, E. A. Dratz, Solvent effects on the spectra of retinal Schiff bases—I. models for the bathochromic shift of the chromophore spectrum in visual pigments. *Photochem. Photobiol.* **25**, 277–286 (1977).
30. M. M. LaVail, B.-A. Battelle, Influence of eye pigmentation and light deprivation on inherited retinal dystrophy in the rat. *Exp. Eye Res.* **21**, 167–192 (1975).
31. T. J. van den Berg, J. K. IJspeert, P. W. de Waard, Dependence of intraocular straylight on pigmentation and light transmission through the ocular wall. *Vision Res.* **31**, 1361–1367 (1991).
32. S. Nusinowitz *et al*., Electroretinographic evidence for altered phototransduction gain and slowed recovery from photobleaches in albino mice with a MET450 variant in RPE65. *Exp. Eye Res.* **77**, 627–638 (2003).
33. J. S. Penn, T. P. Williams, Photostasis: Regulation of daily photon-catch by rat retinas in response to various cyclic illuminances. *Exp. Eye Res.* **43**, 915–928 (1986).
34. T. D. Lamb, E. N. Pugh Jr., Dark adaptation and the retinoid cycle of vision. *Prog. Retin. Eye Res.* **23**, 307–380 (2004).
35. A. Wenzel, C. E. Reme, T. P. Williams, F. Hafezi, C. Grimm, The Rpe65 Leu450Met variation increases retinal resistance against light-induced degeneration by slowing rhodopsin regeneration. *J. Neurosci.* **21**, 53–58 (2001).
36. A. L. Lyubarsky *et al*., Mole quantity of RPE65 and its productivity in the generation of 11-cis-retinal from retinyl esters in the living mouse eye. *Biochemistry* **44**, 9880–9888 (2005).
37. M. Jin, S. Li, W. N. Moghrabi, H. Sun, G. H. Travis, Rpe65 is the retinoid isomerase in bovine retinal pigment epithelium. *Cell* **122**, 449–459 (2005).
38. T. M. Redmond *et al*., Mutation of key residues of RPE65 abolishes its enzymatic role as isomerohydrolase in the visual cycle. *Proc. Natl. Acad. Sci. U.S.A.* **102**, 13658–13663 (2005).
39. G. Moiseyev *et al*., RPE65 is an iron(II)-dependent isomerohydrolase in the retinoid visual cycle. *J. Biol. Chem.* **281**, 2835–2840 (2006).
40. T. M. Redmond *et al*., Rpe65 is necessary for production of 11-cis-vitamin A in the retinal visual cycle. *Nat. Genet.* **20**, 344–351 (1998).
41. J. C. Saari *et al*., Visual cycle impairment in cellular retinaldehyde binding protein (CRALBP) knockout mice results in delayed dark adaptation. *Neuron* **29**, 739–748 (2001).
42. Y. Xue *et al*., CRALBP supports the mammalian retinal visual cycle and cone vision. *J. Clin. Invest.* **125**, 727–738 (2015).
43. E. Z. Szuts, F. I. Harosi, Solubility of retinoids in water. *Arch. Biochem. Biophys.* **287**, 297–304 (1991).
44. J. L. Napoli, Cellular retinoid binding-proteins, CRBP, CRABP, FABP5: Effects on retinoid metabolism, function and related diseases. *Pharmacol. Ther.* **173**, 19–33 (2017).
45. R. S. Molday, M. Zhong, F. Quazi, The role of the photoreceptor ABC transporter ABCA4 in lipid transport and Stargardt macular degeneration. *Biochim. Biophys. Acta* **1791**, 573–583 (2009).
46. J. J. Kaylor *et al*., Identification of DES1 as a vitamin A isomerase in Müller glial cells of the retina. *Nat. Chem. Biol.* **9**, 30–36 (2013).
47. P. D. Kiser, M. Golczak, K. Palczewski, Chemistry of the retinoid (visual) cycle. *Chem. Rev.* **114**, 194–232 (2014).

48. M. J. Mattapallil *et al*., The Rd8 mutation of the Crb1 gene is present in vendor lines of C57BL/6N mice and embryonic stem cells, and confounds ocular induced mutant phenotypes. *Invest. Ophthalmol. Vis. Sci.* **53**, 2921–2927 (2012).
49. P. D. Kiser *et al*., Conditional deletion of Des1 in the mouse retina does not impair the visual cycle in cones. *FASEB J.* **33**, 5782–5792 (2019).
50. J. von Lintig, P. D. Kiser, M. Golczak, K. Palczewski, The biochemical and structural basis for trans-to-cis isomerization of retinoids in the chemistry of vision. *Trends Biochem. Sci.* **35**, 400–410 (2010).
51. Q. Zhang *et al*., Disruption of RPGR protein interaction network is the common feature of RPGR missense variations that cause XLRP. *Proc. Natl. Acad. Sci. U.S.A.* **116**, 1353–1360 (2019).
52. N. Froger *et al*., Taurine: The comeback of a neutraceutical in the prevention of retinal degenerations. *Prog. Retin. Eye Res.* **41**, 44–63 (2014).
53. H. Ripps, W. Shen, Review: Taurine: A "very essential" amino acid. *Mol. Vis.* **18**, 2673–2686 (2012).
54. S. G. Jacobson, C. M. Kemp, F. X. Borruat, M. H. Chaitin, D. J. Faulkner, Rhodopsin topography and rod-mediated function in cats with the retinal degeneration of taurine deficiency. *Exp. Eye Res.* **45**, 481–490 (1987).
55. E. L. Berson, K. C. Hayes, A. R. Rabin, S. Y. Schmidt, G. Watson, Retinal degeneration in cats fed casein. II. Supplementation with methionine, cysteine, or taurine. *Invest. Ophthalmol.* **15**, 52–58 (1976).
56. S. Y. Schmidt, E. L. Berson, K. C. Hayes, Retinal degeneration in cats fed casein. I. Taurine deficiency. *Invest. Ophthalmol.* **15**, 47–52 (1976).
57. B. Heller-Stilb *et al*., Disruption of the taurine transporter gene (taut) leads to retinal degeneration in mice. *FASEB J.* **16**, 231–233 (2002).
58. H. Pasantes-Morales, R. M. Ademe, O. Quesada, Protective effect of taurine on the light-induced disruption of isolated frog rod outer segments. *J. Neurosci. Res.* **6**, 337–348 (1981).
59. H. Pasantes-Morales, C. Cruz, Taurine and hypotaurine inhibit light-induced lipid peroxidation and protect rod outer segment structure. *Brain Res.* **330**, 154–157 (1985).
60. H. T. Orr, A. I. Cohen, J. A. Carter, The levels of free taurine, glutamate, glycine and gamma-amino butyric acid during the postnatal development of the normal and dystrophic retina of the mouse. *Exp. Eye Res.* **23**, 377–384 (1976).
61. J. Fan, B. Rohrer, G. Moiseyev, J. X. Ma, R. K. Crouch, Isorhodopsin rather than rhodopsin mediates rod function in RPE65 knock-out mice. *Proc. Natl. Acad. Sci. U.S.A.* **100**, 13662–13667 (2003).
62. T. M. Redmond, E. Poliakov, S. Kuo, P. Chander, S. Gentleman, RPE65, visual cycle retinol isomerase, is not inherently 11-cis-specific: Support for a carbocation mechanism of retinol isomerization. *J. Biol. Chem.* **285**, 1919–1927 (2010).
63. C. S. Bolze *et al*., Human cellular retinaldehyde-binding protein has secondary thermal 9-cis-retinal isomerase activity. *J. Am. Chem. Soc.* **136**, 137–146 (2014).
64. R. C. C. St George, The interplay o light and heat in bleaching rhodopsin. *J. Gen. Physiol.* **35**, 495–517 (1952).
65. J. F. Ashmore, G. Falk, Dark noise in retinal bipolar cells and stability of rhodopsin in rods. *Nature* **270**, 69–71 (1977).
66. R. R. Birge, B. M. Pierce, Theoretical-analysis of the 2-photon properties of linear polyenes and the visual chromophores. *J. Chem. Phys.* **70**, 165–178 (1979).
67. K. Schulten, U. Dinur, B. Honig, The spectra of carbonium-ions, cyanine dyes, and protonated schiff-base polyenes. *J. Chem. Phys.* **73**, 3927–3935 (1980).
68. R. D. J. Froese, I. Komaromi, K. S. Byun, K. Morokuma, Theoretical studies of protonated and non-protonated Schiff bases of retinal: Ground state structures and energies of the all-trans, 13-cis, 11-cis, 9-cis, 6,7-cis, and 6-s-cis isomers. *Chem. Phys. Lett.* **272**, 335–340 (1997).
69. O. Quesada, A. Picones, H. Pasantes-Morales, Effect of light deprivation on the ERG responses of taurine-deficient rats. *Exp. Eye Res.* **46**, 13–20 (1988).
70. R. N. Rasmussen, C. Lagunas, J. Plum, R. Holm, C. U. Nielsen, Interaction of GABA-mimetics with the taurine transporter (TauT, Slc6a6) in hyperosmotic treated Caco-2, LLC-PK1 and rat renal SKPT cells. *Eur. J. Pharm. Sci.* **82**, 138–146 (2016).
71. S. R. Kim *et al*., Rpe65 Leu450Met variant is associated with reduced levels of the retinal pigment epithelium lipofuscin fluorophores A2E and iso–A2E. *Proc. Natl. Acad. Sci. U.S.A.* **101**, 11668–11672 (2004).
72. A. M. Petrosian, J. E. Haroutounian, L. V. Zueva, Tauret. A taurine-related endogenous substance in the retina and its role in vision. *Adv. Exp. Med. Biol.* **403**, 333–342 (1996).
73. J. R. Lima de Carvalho Jr. *et al*., Effects of deficiency in the *RLBP1*-encoded visual cycle protein CRALBP on visual dysfunction in humans and mice. *J. Biol. Chem.* **295**, 6767–6780 (2020).
74. M. A. Kane, A. E. Folias, J. L. Napoli, HPLC/UV quantitation of retinal, retinol, and retinyl esters in serum and tissues. *Anal. Biochem.* **378**, 71–79 (2008).
75. X. Wang, D. Chi, G. Su, L. Li, L. Shao, Determination of taurine in biological samples by high-performance liquid chromatography using 4-fluoro-7-nitrobenzofurazan as a derivatizing agent. *Biomed. Environ. Sci.* **24**, 537–542 (2011).